PHYSICAL REVIEW B VOLUME 23, NUMBER 9 1 MAY 1981

# Electronic structure and Mössbauer quadrupole splittings in iron (II) pentacyanides

M. Braga
*Departamento de Física, Universidade Federal de Pernambuco, 50000-Recife, Brasil*

A. C. Pavão
*Departamento de Física and Departamento de Química, Universidade Federal de Pernambuco, 50000-Recife, Brasil*

J. R. Leite
*Instituto de Física, Universidade de São Paulo, CP 20516-São Paulo, Brasil*

(Received 5 November 1980)

Multiple-scattering calculations have been performed for the isoelectronic series of the iron (II) pentacyanides $Fe(CN)_5NO^{2-}$, $Fe(CN)_5CO^{3-}$, and $Fe(CN)_5N_2^{3-}$. Fe $3d$ and $4p$ populations and total electron densities at the iron nucleus derived from these calculations are used to interpret experimental Mössbauer quadrupole splittings and electric field gradients at the iron nucleus. Covalency effects involving the Fe $3d$ and $4p$ orbitals ($\pi$ back donation and $\sigma$ donation, respectively) are found to play a major role in the calculated field gradients. The calculated quadrupole splittings are found to be in good agreement with the experimental values.

## I. INTRODUCTION

Hyperfine interactions in Mössbauer spectroscopy are known to be a very useful source of information about the electronic environment at the Mössbauer nucleus. In the present paper we describe the interpretation of experimental Mössbauer quadrupole splittings (QS) using the theoretical results derived from self-consistent-field–molecular-orbital (SCF-MO) calculations. Electric quadrupole interaction occurs if there is a nuclear quadrupole moment and simultaneously a nonvanishing electric field gradient (EFG) at the nucleus. The total splitting of degenerate nuclear energy levels as a consequence of this interaction is given by

$$\Delta E_Q = \tfrac{1}{2} e^2 Q q (1 + \tfrac{1}{3}\eta)^{1/2} \ , \tag{1}$$

$$q = \frac{V_{zz}}{e} \ , \tag{2}$$

$$\eta = \frac{V_{xx} - V_{yy}}{V_{zz}} \ , \tag{3}$$

where $V_{xx}$, $V_{yy}$, and $V_{zz}$ are the components of the EFG tensor obtained from the diagonalization of the EFG tensor $V_{pq} = \partial^2 V / \partial p \, \partial q$ ($p,q = x,y,z$) and $Q$ is the nuclear quadrupole moment. The EFG is therefore specified by two different parameters: $q$ and $\eta$ (the "asymmetry parameter"). In the case of compounds with a fourfold or threefold symmetry axis, $V_{xx} = V_{yy}$ and $\eta$ becomes zero. Equation (1) may be rewritten as

$$\Delta E_Q = \tfrac{1}{2} e^2 Q q \ . \tag{4}$$

Three different sources are usually considered as contributing to the total EFG at the nucleus[1]: (a) charges on the lattice surrounding the Mössbauer atom in a noncubic symmetry, (b) noncubic charge distribution in the valence shells of the Mössbauer atom, (c) core polarization. It is clear that this contribution is a consequence of the influence of the other two on the core electrons, otherwise these are in spherically symmetric shells and produce no field gradient. Taking into account these contributions and for $C_{4v}$ symmetry, the EFG is conveniently expressed as

$$q = (1 - R) q_{\text{val}} + (1 - \gamma_\infty) q_{\text{lat}} \ , \tag{5}$$

where $q_{\text{val}}$ and $q_{\text{lat}}$ refers to the valence and lattice contributions, respectively, and $R$ and $\gamma_\infty$ are the Sternheimer polarization factors.[1]

Previous studies have demonstrated that the multiple-scattering $X\alpha$ (MS-$X\alpha$) cluster method[2] can be successfully applied to study hyperfine interactions in a wide variety of systems such as the iron fluorides,[3] the ferrocyanide,[4] and ferricyanide[5] ions, the ferrates[6] and dithioferrates,[7] interstitial hydrogen atom in alkali-earth fluorides,[8] color centers in KCl,[9] and recently the hydrogen and transition-metal atoms isolated in a crystalline argon matrix.[10–12] The calculated MO wave functions, total electron densities at the nucleus, and atomic populations have been used to interpret experimental hyperfine parameters. However, the MS calculations reported earlier have been mainly concerned with the iron isomer shift (and the iron isomer shift calibration constant) and the hyperfine field at the nucleus. No attempt has

 

ever been made to use MS calculations to interpret experimental Mössbauer QS. On the other hand, the MS method has proved to be valuable in the description of the electronic structure and bonding of transition metal complexes containing $\pi$-acceptor ligands such as the cyanides[4,5] and the carbonyl and nitrogenyl groups.[13]

In this paper we shall apply the MS-cluster method to the study of Mössbauer QS in the isoelectronic series of the iron (II) pentacyanides $Fe(CN)_5NO^{2-}$, $Fe(CN)_5CO^{3-}$, and $Fe(CN)_5N_2^{3-}$. From the calculated MO wave functions and orbital populations we obtain the EFG at the iron nucleus as well as the energy shift resulting from the electric quadrupole interaction. The present compounds are particularly well suited for study. Numerous experimental studies of the Mössbauer spectrum of the nitroprusside ion with single crystals and in frozen solutions have been carried out.[14,15] The pentacyanocarbonyl and pentacyanonitrogenyl complexes have also been investigated (Refs. 16 and 17, respectively). Covalency effects involving the Fe $3d$ electrons have been considered to play a major role in the bonding of these complexes.[14,16,18,19] A detailed analysis of the different contributions to the EFG in the iron (II) pentacyanide series using an iterative extended Hückel method has been carried out by Trautwein and Harris.[20]

It has been found[14(b)] that the QS of the sodium nitroprusside is temperature independent over a wide temperature region. No such experimental information is available for the other complexes. However, since most of the iron (II) pentacyanides investigated were found to be temperature independent, one can safely assume that all the compounds we are considering behave in the same way. We therefore feel justified to limit our calculations to the self-consistent study of the ground state, the effect of the low-lying excited electronic states being neglected. Furthermore, experimental data[14(b)] indicate a negligible contribution of the lattice charges to the field gradient. A cluster consisting of the iron atom and its nearest neighbors would then be a realistic model to describe hyperfine interactions in iron (II) pentacyanides. Covalency effects involving the iron $3d$ and $4p$ valence orbitals play a fundamental role in the calculated EFG and QS. Core polarization (mainly of the $3p$ orbital) is found to be completely negligible.

## II. COMPUTATIONAL METHOD

The MS method[2] with Slater's $X\alpha$ exchange has been applied to the following clusters: $Fe(CN)_5NO^{2-}$, $Fe(CN)_5CO^{3-}$, and $Fe(CN)_5N_2^{3-}$. For the nitrosyl cluster the experimental distances were used.[18] For the carbonyl and nitrogenyl clusters, we assume the Fe–CN distance (for the equatorial and axial CN groups) to be the same as in the nitrosyl cluster. For the Fe–CO distance, an intermediate value between the Fe–NO and the Fe–CN distances was used. The same criteria was used for the $Fe-N_2$ distance. The C–O and N–N distances were taken to be the same as in the free molecules. The values of the atomic exchange parameter $\alpha$ used in the present calculations were taken from Schwarz.[21] In the outer and intersphere regions a weighted average of the atomic values has been used.

The MS method has been previously discussed in a number of papers.[2] The partial wave expansions in the different atomic spheres were chosen according the following values of $l$ (the spherical harmonic orbital quantum number): for the iron atom and in the outer region we are using $l=0$, 1, and 2 for orbitals of $a_1$ symmetry, $l=4$ for $a_2$ symmetry, $l=2$ for $b_1$ and $b_2$ symmetries and $l=1$, 2 for the $e$ symmetry; for the ligand spheres we are using $l=0$ and/or 1 for all the symmetries. Calculations have been carried out to self-consistency, all the electrons (core + valence) included in each SCF cycle. Uniformly charged spheres (Watson spheres[22]) with charges of the same magnitude and opposite sign to those of the clusters have also been used.

The unusually short Fe–NO distance makes the muffin-tin nonoverlapping spheres partitioning of the cluster space to be a nonsuitable representation of the true crystal potential. It leads to an excessively small N sphere and too large an O sphere, which makes the model unphysical. The same consideration is approximately true for the carbonyl and nitrogenyl systems but the problem is not so serious there. In addition, previous muffin-tin nonoverlapping-spheres calculations for the ferrocyanide[4] and ferricyanide[5] clusters showed that a large fraction of the electronic charge lies in the interatomic region. In the present calculation we have used ligand spheres whose radii were increased in about 40% from the values of the Pauling's[23] covalent radii used in previous MS calculations.[4,5] Large overlaps, as we are using, have been previously used[24] and the calculated properties for the free ligand molecules were found to be in excellent agreement with the experimental data. On the other hand, it is known that smaller transition metal radius leads to a better description of the $3d$ levels and crystal field splittings.[3,4] We have therefore reduced the iron sphere radius from the value reported in Ref. 4 in such a way that the resulting sphere does not overlap the CN spheres but the NO (CO or $N_2$). This potential model was adopted after a number of tests in which different criteria and types of overlapping- and nonoverlapping-spheres models were used. It is further found that this model leads to an ordering of the higher occupied and lower unoccupied energy levels in agreement with the optical spectrum.[18] It is worth it to point out that in the calculation program the potential contribution from the different atomic

spheres has been decreased by a volume factor to account for the overlap between the spheres and in a way that the charge density in the overlap region is counted only once in the calculation of the potential.[25]

From the calculated MO wave functions we have derived the atomic occupancies by using the Larsson's technique.[26] The atomic populations are defined as

$$P_l = \sum_i n_i \frac{C_{il}^2}{K_l^2} \quad , \tag{6}$$

where $n_i$ is the population of the orbital $i$, $C_{il}$ are the expansion coefficients of the partial wave representation for the MO in the different atomic spheres, and $K_l$ is the amplitude of an atomic orbital used as reference orbital.

## III. ENERGY LEVELS

In Fig. 1 we are giving the calculated energy spectra for the $Fe(CN)_5NO^{2-}$, $Fe(CN)_5CO^{3-}$, and $Fe(CN)_5N_2^{3-}$ clusters. We have only included some of the upper occupied and lower unoccupied levels.

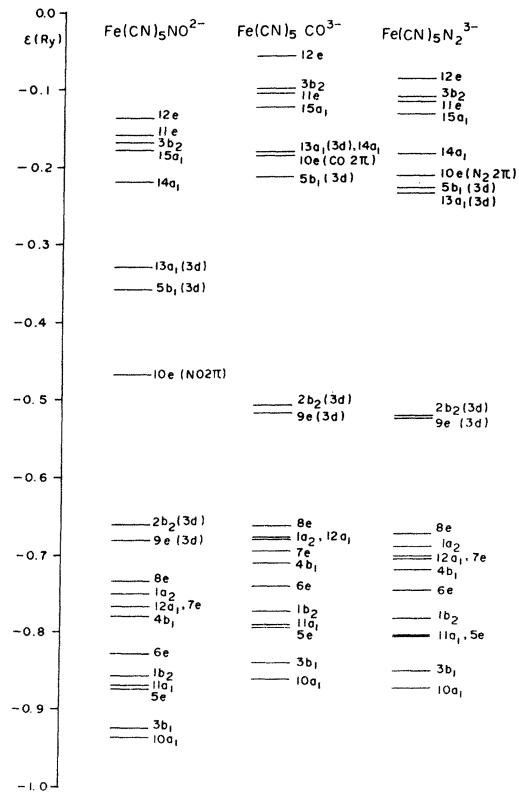


FIG. 1. Upper occupied and lower unoccupied energy levels for the $Fe(CN)_5NO^{2-}$, $Fe(CN)_5CO^{3-}$, and $Fe(CN)_5N_2^{3-}$ clusters.

The $\sigma$ orbitals of the four equatorial CN groups (hereafter referred as $C_eN_e$) are distributed on the $a_1$, $b_1$, and $e$ representations and the $\pi$ orbitals on the $a_1$, $a_2$, $b_1$, $b_2$, and $e$. The $\sigma$ and $\pi$ orbitals of the axial CN ($C_aN_a$) and NO (CO and $N_2$) groups are found in the $a_1$ and $e$ symmetries, respectively. The orbital energies and charge distributions within the different muffin-tin regions are given in Tables I–III. Fe populations for the valence orbitals (including the $3s, 3p$ usually regarded as core orbitals) are given in Table IV. To determine the $K_l$ coefficients in Eq. (6) we have used the $3d^64s^{0+2}$ configuration for atomic iron. Fe $4p$ levels are very poorly described in a Hartree-Fock-Slater calculation; i.e., they are too diffuse orbitals. Therefore, the use of the $K_{4p}$ coefficient obtained from such an atomic calculation would lead to an excessively large $4p$ population for the clusters, which in turn results in too low values for the calculated field gradients and QS. A most reliable $4p$ reference function can be obtained by requiring the total $4p$ occupancy in the nitroprusside cluster to be equal to the total $4p$ occupancy resulting from some accurate MO calculation. For this purpose, we have chosen the MO calculation reported by Fenske and DeKock.[19] It is important to note that our fitting leads to partial $4p_z$ and $4p_x$, $4p_y$ populations completely different from the values obtained in Ref. 19 (and in any other MO calculation available). Since the calculated EFG does not depend on the total $4p$ charge but the difference between the $4p_z$ and $4p_x$, $4p_y$ populations we feel that our results are not critically dependent on the way we are getting the $4p$ reference function.

In the $Fe(CN)_5NO^{2-}$ cluster, the $1a_1$ and the $2a_1$, $1e$ orbitals correspond to the iron $3s$ and $3p$ orbitals, respectively. The $3a_1$, $6a_1$, $7a_1$, and $3e$ are NO $3\sigma$, $4\sigma$, $5\sigma$, and $1\pi$ orbitals, respectively, with different degrees of iron $3d$, $4s$, and $4p$ admixture, particularly in the $6a_1$ and $7a_1$ levels. The $5a_1$, $9a_1$, $11a_1$, and $8e$ orbitals correspond to the $C_aN_a$ $3\sigma$, $4\sigma$, $5\sigma$, and $1\pi$, respectively, with some iron $3d$ and $4p$ character in the $9a_1$, $11a_1$, and $8e$. The $4a_1$, $2e$, and $1b_1$ orbitals correspond to $C_eN_e$ $3\sigma$; $8a_1$, $2b_1$, and $4e$ to $C_eN_e$ $4\sigma$; $10a_1$, $3b_1$, and $5e$ to $C_eN_e$ $5\sigma$; and $1b_2$, $6e$, $4b_1$, $12a_1$, $7e$, and $1a_2$ to $C_eN_e$ $1\pi$. Large iron $4s$, $4p$, and $3d$ components appear in the $8a_1$ (54% of one electron), $5e$ (55%), and $6e$ (63%) orbitals, respectively. Some iron $3d$ character is also present in the $8a_1$ and $8e$; iron $4s$ in the $10a_1$ and iron $4p$ in $12a_1$, $4e$, and $7e$. Large iron $3d$ components are also found in the $2b_1$, $3b_1$, and $1b_2$ levels. Finally, the $9e$ and $2b_2$ are the crystal-field Fe $3d$ orbitals with an important ligand admixture in the former (mainly NO $1\pi$ and $2\pi$ and some $C_aN_a$ and $C_eN_e$ $1\pi$ and $2\pi$). The $2b_2$ is largely a nonbonding orbital (this is also true for the carbonyl and nitrogenyl clusters).

The electronic structure of the $Fe(CN)_5CO^{3-}$ and $Fe(CN)_5N_2^{3-}$ clusters is roughly the same as in the

TABLE I. Orbital energies and integrated charge density (in % one-electron charge) for $Fe(CN)_5NO^{2-}$. $C_e$, $N_e$ and $C_a$, $N_a$ are the equatorial and axial CN groups, respectively. Total charge: Fe sphere: 25.06; $C_e$ sphere (each): 5.05; $N_e$ sphere: 5.73; $C_a$ sphere: 5.08; $N_a$ sphere: 5.73; N sphere: 5.81; O sphere: 6.63; intersphere region: 16.08; outer sphere: 0.53.

| Orbital | Orbital energy (−Ry) | Charge in muffin-tin sphere | | | | | | | | |
|---|---|---|---|---|---|---|---|---|---|---|
| | | Fe | $C_e$ | $N_e$ | $C_a$ | $N_a$ | N | O | Interatomic | Outersphere |
| $1a_1$ | 6.808 | 99.69 | 0.0 | 0.0 | 0.0 | 0.0 | 0.04 | 0.0 | 0.26 | 0.0 |
| $2a_1$ | 4.480 | 98.91 | 0.0 | 0.0 | 0.05 | 0.0 | 0.41 | 0.0 | 0.63 | 0.0 |
| $1e$ | 4.474 | 99.14 | 0.03 | 0.0 | 0.0 | 0.0 | 0.0 | 0.0 | 0.75 | 0.0 |
| $3a_1$ | 2.625 | 0.04 | 0.0 | 0.0 | 0.0 | 0.0 | 42.80 | 56.35 | 0.79 | 0.02 |
| $4a_1$ | 2.132 | 0.0 | 10.37 | 11.59 | 0.01 | 0.01 | 0.0 | 0.0 | 12.05 | 0.06 |
| $2e$ | 2.131 | 0.0 | 10.35 | 11.59 | 0.0 | 0.0 | 0.0 | 0.0 | 12.17 | 0.05 |
| $1b_1$ | 2.130 | 0.0 | 10.32 | 11.57 | 0.0 | 0.0 | 0.0 | 0.0 | 12.36 | 0.08 |
| $5a_1$ | 2.061 | 0.0 | 0.0 | 0.0 | 41.39 | 47.08 | 0.0 | 0.0 | 11.42 | 0.07 |
| $6a_1$ | 1.595 | 10.73 | 0.05 | 0.01 | 0.23 | 0.01 | 42.71 | 27.59 | 18.29 | 0.18 |
| $7a_1$ | 1.352 | 11.01 | 0.06 | 0.01 | 0.65 | 0.03 | 29.44 | 45.24 | 12.90 | 0.44 |
| $3e$ | 1.123 | 3.40 | 0.49 | 0.11 | 0.0 | 0.0 | 32.43 | 33.52 | 28.19 | 0.05 |
| $8a_1$ | 1.088 | 16.51 | 10.26 | 1.91 | 1.63 | 0.05 | 0.63 | 0.02 | 31.83 | 0.17 |
| $2b_1$ | 1.021 | 31.79 | 9.15 | 2.85 | 0.0 | 0.0 | 0.0 | 0.0 | 19.53 | 0.69 |
| $4e$ | 0.983 | 1.31 | 4.74 | 11.70 | 0.28 | 0.12 | 0.37 | 1.26 | 29.41 | 1.48 |
| $9a_1$ | 0.957 | 7.66 | 0.75 | 0.51 | 24.56 | 30.52 | 0.91 | 0.38 | 29.38 | 1.53 |
| $10a_1$ | 0.934 | 3.40 | 3.03 | 14.66 | 0.11 | 0.62 | 0.0 | 0.0 | 21.98 | 3.11 |
| $3b_1$ | 0.926 | 10.25 | 3.10 | 13.86 | 0.0 | 0.0 | 0.0 | 0.0 | 17.67 | 4.22 |
| $5e$ | 0.875 | 5.12 | 9.07 | 5.73 | 2.48 | 1.47 | 0.02 | 0.87 | 29.66 | 1.18 |
| $11a_1$ | 0.871 | 9.05 | 1.37 | 0.97 | 20.42 | 33.36 | 0.76 | 0.28 | 24.49 | 2.26 |
| $1b_2$ | 0.858 | 18.83 | 6.78 | 5.16 | 0.0 | 0.0 | 0.0 | 0.0 | 32.85 | 0.53 |
| $6e$ | 0.828 | 17.22 | 5.26 | 4.36 | 3.57 | 2.75 | 0.02 | 7.22 | 30.52 | 0.26 |
| $4b_1$ | 0.780 | 0.04 | 0.46 | 8.46 | 0.0 | 0.0 | 0.0 | 0.0 | 59.89 | 4.37 |
| $12a_1$ | 0.767 | 3.31 | 5.40 | 5.57 | 10.19 | 1.53 | 1.65 | 2.29 | 31.05 | 0.15 |
| $7e$ | 0.766 | 0.68 | 7.83 | 8.07 | 1.27 | 1.42 | 0.03 | 0.57 | 32.39 | 0.02 |
| $1a_2$ | 0.780 | 0.03 | 7.31 | 10.10 | 0.0 | 0.0 | 0.0 | 0.0 | 29.17 | 1.18 |
| $8e$ | 0.734 | 3.27 | 2.91 | 3.37 | 16.26 | 22.53 | 0.15 | 0.47 | 32.15 | 0.05 |
| $9e$ | 0.681 | 49.27 | 0.94 | 1.88 | 3.43 | 8.08 | 2.70 | 6.67 | 18.06 | 0.50 |
| $2b_2$[a] | 0.661 | 70.00 | 0.78 | 3.37 | 0.0 | 0.0 | 0.0 | 0.0 | 12.97 | 0.42 |
| $10e$ | 0.468 | 17.58 | 0.50 | 0.04 | 0.01 | 0.20 | 37.87 | 22.79 | 19.29 | 0.09 |
| $5b_1$ | 0.358 | 56.79 | 7.26 | 0.90 | 0.0 | 0.0 | 0.0 | 0.0 | 10.19 | 0.38 |
| $13a_1$ | 0.329 | 60.18 | 2.30 | 0.39 | 10.05 | 1.30 | 4.99 | 1.40 | 10.76 | 0.59 |

[a]Highest occupied level.

nitroprusside cluster. Even though some inversions between the energy levels occur, the main orbital features are the same (see Tables II and III). However, some significant differences in the distribution of the metal $3d$, $4s$, and $4p$ components are found. In the $Fe(CN)_5CO^{3-}$ cluster, the iron $4s$ component is mainly concentrated in the $7a_1$ CO $5\sigma$ level with 77% of one electron. Some iron $4s$ character is also found in the $10a_1$ $C_eN_e$ $5\sigma$ orbital. This situation resembles what has previously been found for the $Ni(CO)_4$.[13] Large iron $4p$ character appears in the $5e$ (52%), $3e$, and $11a_1$ orbitals. Iron $3d$ component is important in the $8a_1$ level (30%), $6e$, and $11a_1$. In the $Fe(CN)_5N_2^{3-}$ cluster, the iron $4s$ charge is not concentrated in one level but distributed among the $6a_1$ (27%), $7a_1$ (20%), $8a_1$ (29%), and $10a_1$ (10%) orbitals. Iron $3d$ and $4p$ character appears in the $6e$, $8a_1$, $11a_1$, and $5e$ (50%), $3e$, $7e$, $6a_1$, $9a_1$, $11a_1$ orbitals, respectively. As in the nitroprusside cluster, large iron $3d$ component is also present in the $2b_1$, $3b_1$, and $1b_2$ levels in both clusters.

From the former description of the structure of the calculated energy levels it is seen that the significant metal charge (involving the iron $4s$, $4p$, and $3d_{z^2}$, $3d_{x^2-y^2}$ orbitals) found in most of the ligand MO is largely donated from filled $\sigma$-ligand orbitals. Some ligand-to-metal $\pi$ donation may also be found. Since the structure of the $a_1$ and $e$ orbitals is further complicated because of the $\sigma$-$\pi$ mixing it is very hard to determine the extension of the ligand $\pi$ donation. Ligand-to-metal $\sigma$ donation is by far the most important contribution to the stability of the bond. As it

TABLE II. Oribtal energies and integrated charge density (in % of one electron charge) for $Fe(CN)_5CO^{3-}$. $C_e$, $N_e$ and $C_a$, $N_a$ are the equatorial and axial CN groups, respectively. Total charge: Fe sphere: 25.02; $C_e$ sphere: 5.03; $N_e$ sphere: 5.75; $C_a$ sphere: 5.08; $N_a$ sphere: 5.76; C sphere: 5.04; O sphere: 6.65; intersphere region: 16.71; outer region: 0.60.

| Orbital | Orbital energies (−Ry) | Charge in muffin-tin sphere | | | | | | | | |
|---|---|---|---|---|---|---|---|---|---|---|
| | | Fe | $C_e$ | $N_e$ | $C_a$ | $N_a$ | C | O | Interatomic | Outersphere |
| $1a_1$ | 6.620 | 99.69 | 0.0 | 0.0 | 0.0 | 0.0 | 0.02 | 0.0 | 0.27 | 0.0 |
| $2a_1$ | 4.288 | 99.04 | 0.0 | 0.0 | 0.05 | 0.0 | 0.18 | 0.0 | 0.72 | 0.0 |
| $1e$ | 4.287 | 99.09 | 0.03 | 0.0 | 0.0 | 0.0 | 0.0 | 0.0 | 0.80 | 0.0 |
| $3a_1$ | 2.389 | 0.01 | 0.0 | 0.0 | 0.0 | 0.0 | 36.17 | 56.14 | 7.63 | 0.05 |
| $4a_1$ | 2.048 | 0.0 | 10.36 | 11.70 | 0.02 | 0.02 | 0.0 | 0.0 | 11.67 | 0.07 |
| $2e$ | 2.047 | 0.0 | 10.33 | 11.71 | 0.0 | 0.0 | 0.0 | 0.0 | 11.79 | 0.05 |
| $1b_1$ | 2.046 | 0.0 | 10.29 | 11.68 | 0.0 | 0.0 | 0.0 | 0.0 | 12.00 | 0.10 |
| $5a_1$ | 1.983 | 0.0 | 0.0 | 0.01 | 41.34 | 47.43 | 0.0 | 0.0 | 11.10 | 0.08 |
| $6a_1$ | 1.232 | 0.87 | 0.07 | 0.01 | 0.06 | 0.0 | 18.06 | 61.47 | 18.18 | 1.00 |
| $7a_1$ | 1.051 | 12.67 | 4.71 | 0.87 | 5.25 | 0.74 | 21.31 | 6.34 | 31.16 | 0.24 |
| $8a_1$ | 0.949 | 23.37 | 5.02 | 3.02 | 0.43 | 0.01 | 20.38 | 2.26 | 20.86 | 0.54 |
| $3e$ | 0.927 | 1.60 | 4.02 | 8.13 | 0.10 | 0.05 | 6.40 | 10.65 | 31.74 | 0.88 |
| $2b_1$ | 0.920 | 14.68 | 7.15 | 7.90 | 0.0 | 0.0 | 0.0 | 0.0 | 22.75 | 2.38 |
| $4e$ | 0.895 | 1.35 | 0.90 | 4.90 | 0.09 | 0.04 | 14.81 | 31.47 | 27.83 | 1.18 |
| $9a_1$ | 0.881 | 2.07 | 0.58 | 0.79 | 16.99 | 40.32 | 2.88 | 0.57 | 29.27 | 2.45 |
| $10a_1$ | 0.863 | 6.83 | 4.08 | 12.38 | 0.35 | 2.05 | 0.68 | 0.04 | 21.31 | 2.92 |
| $3b_1$ | 0.841 | 20.75 | 6.32 | 8.82 | 0.0 | 0.0 | 0.0 | 0.0 | 15.77 | 2.92 |
| $5e$ | 0.795 | 4.41 | 9.07 | 4.82 | 2.98 | 1.98 | 0.28 | 2.02 | 31.68 | 1.11 |
| $11a_1$ | 0.791 | 7.95 | 2.50 | 1.95 | 21.43 | 20.97 | 1.33 | 0.28 | 28.32 | 1.90 |
| $1b_2$ | 0.773 | 8.51 | 7.21 | 6.40 | 0.0 | 0.0 | 0.0 | 0.0 | 12.39 | 0.40 |
| $6e$ | 0.741 | 5.98 | 5.90 | 5.92 | 3.70 | 3.40 | 0.19 | 4.62 | 34.39 | 0.42 |
| $4b_1$ | 0.710 | 0.07 | 0.41 | 7.64 | 0.0 | 0.0 | 0.0 | 0.0 | 63.08 | 4.65 |
| $7e$ | 0.694 | 0.74 | 7.47 | 7.84 | 2.10 | 2.52 | 0.0 | 0.58 | 32.84 | 0.01 |
| $1a_2$ | 0.680 | 0.03 | 6.96 | 10.29 | 0.0 | 0.0 | 0.0 | 0.0 | 29.63 | 1.34 |
| $12a_1$ | 0.677 | 2.63 | 3.97 | 6.91 | 15.52 | 2.30 | 5.65 | 0.41 | 29.87 | 0.10 |
| $8e$ | 0.662 | 1.02 | 3.17 | 2.52 | 17.08 | 25.83 | 0.01 | 0.10 | 33.11 | 0.07 |
| $9e$ | 0.516 | 71.90 | 0.11 | 1.49 | 0.29 | 3.24 | 0.99 | 3.07 | 13.71 | 0.38 |
| $2b_2$[a] | 0.506 | 76.59 | 0.08 | 2.58 | 0.0 | 0.0 | 0.0 | 0.0 | 12.38 | 0.40 |
| $5b_1$ | 0.213 | 62.30 | 5.87 | 0.79 | 0.0 | 0.0 | 0.0 | 0.0 | 10.33 | 0.73 |
| $10e$ | 0.185 | 8.40 | 0.74 | 0.68 | 0.05 | 0.05 | 30.21 | 18.58 | 35.93 | 1.12 |
| $13a_1$ | 0.181 | 58.87 | 2.28 | 0.28 | 7.60 | 1.15 | 5.54 | 1.16 | 13.47 | 1.98 |

[a]Highest occupied level.

will be discussed (Sec. IV) the relative strength of the $\sigma$ donation from the different ligands plays an important role in the calculated EFG and QS.

The analysis of the lower lying unoccupied energy levels is particularly useful to understand another charge transfer mechanism important for the bonding in the clusters we are considering. In the $Fe(CN)_5NO^{2-}$ cluster, the first unoccupied level is the $10e$ NO $2\pi$ with a large iron $3d$ admixture (86% of one electron). The partial Fe $3d$ occupancy of this level results from the Fe $3d \rightarrow$ NO $2\pi$ back-donation mechanism. The $3d$ charge in the empty NO $2\pi$ antibonding orbital should be roughly equal to the NO $2\pi$ charge in the occupied orbitals belonging to the $e$ representation (this charge is mainly found in the $9e$ level). By mixing the metal $3d$ charge with the $2\pi$ antibonding orbital we are decreasing the antibonding character of the $10e$ level. As a result of this interaction the $10e$ level is considerably lowered in energy and lies in the gap between the occupied crystal field Fe $3d$ orbitals ($5b_1$ and $13a_1$). In the $Fe(CN)_5CO^{3-}$ and $Fe(CN)_5N_2^{3-}$ clusters the situation is rather different. In the former cluster the first empty level is the $5b_1$ Fe $3d$. The $10e$ CO $2\pi$ orbital is now lying in between the unoccupied crystal-field Fe $3d$ levels. The Fe $3d$ component in the $10e$ orbital (44% of one electron) is considerably less than in the nitroprusside cluster and the $10e$ is largely an antibonding orbital. However, the amount of Fe $3d \rightarrow$ CO $2\pi$ back-donated charge is enough to lower this level to a position in between the two empty Fe $3d$ levels. In the $Fe(CN)_5N_2^{3-}$ cluster the $3d$ character of the $10e$

TABLE III. Orbital energies and integrated charge density (in % of one electron charge) for $Fe(CN)_5N_2^{3-}$. $C_e$,$N_e$ and $C_a$, $N_a$ are the equatorial and axial CN groups, respectively. N1 is the nitrogen sphere closest to Fe. Total charge: Fe sphere: 25.02; $C_e$ sphere: 5.04; $N_e$ sphere: 5.74; $C_a$ sphere: 5.07; $N_a$ sphere: 5.75; N1 sphere: 5.84; N2 sphere: 5.71; intersphere region: 16.87; outer region: 0.61.

| Orbital | Orbital energies ($-R_y$) | Charge in muffin-tin sphere | | | | | | | | |
|---|---|---|---|---|---|---|---|---|---|---|
| | | Fe | $C_e$ | $N_e$ | $C_a$ | $N_a$ | N1 | N2 | Interatomic | Outerregion |
| $1a_1$ | 6.634 | 99.73 | 0.0 | 0.0 | 0.0 | 0.0 | 0.0 | 0.0 | 0.24 | 0.0 |
| $2a_1$ | 4.303 | 99.05 | 0.0 | 0.0 | 0.05 | 0.0 | 0.12 | 0.0 | 0.78 | 0.0 |
| $1e$ | 4.302 | 99.11 | 0.03 | 0.0 | 0.0 | 0.0 | 0.0 | 0.0 | 0.78 | 0.0 |
| $3a_1$ | 2.426 | 0.02 | 0.0 | 0.0 | 0.0 | 0.0 | 45.90 | 44.10 | 9.96 | 0.01 |
| $4a_1$ | 2.056 | 0.0 | 10.36 | 11.70 | 0.02 | 0.02 | 0.0 | 0.0 | 11.66 | 0.07 |
| $2e$ | 2.055 | 0.0 | 10.34 | 11.71 | 0.0 | 0.0 | 0.0 | 0.0 | 11.78 | 0.05 |
| $1b_1$ | 2.054 | 0.0 | 10.30 | 11.68 | 0.0 | 0.0 | 0.0 | 0.0 | 11.98 | 0.10 |
| $5a_1$ | 1.995 | 0.0 | 0.01 | 0.01 | 41.38 | 47.38 | 0.0 | 0.0 | 11.12 | 0.08 |
| $6a_1$ | 1.259 | 10.78 | 0.32 | 0.05 | 0.72 | 0.04 | 51.42 | 12.23 | 23.20 | 0.15 |
| $7a_1$ | 1.038 | 2.83 | 1.53 | 0.28 | 1.71 | 0.39 | 8.28 | 51.55 | 26.33 | 1.67 |
| $8a_1$ | 0.997 | 13.30 | 7.91 | 2.50 | 1.18 | 0.53 | 6.11 | 7.65 | 29.13 | 0.47 |
| $3e$ | 0.948 | 2.36 | 2.79 | 3.58 | 0.03 | 0.02 | 23.19 | 15.84 | 32.78 | 0.33 |
| $2b_1$ | 0.930 | 16.05 | 7.41 | 7.38 | 0.0 | 0.0 | 0.0 | 0.0 | 22.61 | 4.60 |
| $4e$ | 0.914 | 1.17 | 2.13 | 9.44 | 0.18 | 0.08 | 12.89 | 10.11 | 27.62 | 1.66 |
| $9a_1$ | 0.896 | 4.34 | 0.69 | 1.59 | 19.84 | 34.57 | 0.70 | 0.60 | 28.36 | 2.48 |
| $10a_1$ | 0.874 | 4.99 | 3.75 | 12.51 | 0.69 | 4.16 | 0.08 | 0.02 | 22.07 | 2.93 |
| $3b_1$ | 0.852 | 19.85 | 5.97 | 9.34 | 0.0 | 0.0 | 0.0 | 0.0 | 15.86 | 3.07 |
| $11a_1$ | 0.806 | 10.89 | 1.85 | 1.35 | 23.20 | 24.91 | 0.55 | 0.18 | 25.40 | 2.05 |
| $5e$ | 0.804 | 4.79 | 8.93 | 4.82 | 3.36 | 2.24 | 0.70 | 1.05 | 31.78 | 1.11 |
| $1b_2$ | 0.783 | 9.00 | 7.19 | 6.32 | 0.0 | 0.0 | 0.0 | 0.0 | 36.18 | 0.76 |
| $6e$ | 0.746 | 5.01 | 6.02 | 6.11 | 3.65 | 3.46 | 1.42 | 3.37 | 34.18 | 0.41 |
| $4b_1$ | 0.719 | 0.07 | 0.41 | 7.66 | 0.0 | 0.0 | 0.0 | 0.0 | 63.07 | 4.60 |
| $12a_1$ | 0.705 | 3.76 | 4.93 | 7.42 | 11.54 | 1.69 | 2.12 | 0.27 | 31.06 | 0.15 |
| $7e$ | 0.702 | 0.75 | 7.49 | 7.79 | 2.15 | 2.59 | 0.16 | 0.54 | 32.68 | 0.01 |
| $1a_2$ | 0.689 | 0.03 | 6.97 | 10.28 | 0.0 | 0.0 | 0.0 | 0.0 | 29.64 | 1.33 |
| $8e$ | 0.673 | 0.99 | 3.37 | 2.52 | 16.88 | 25.42 | 0.01 | 0.12 | 32.95 | 0.07 |
| $9e$ | 0.523 | 74.26 | 0.06 | 1.31 | 0.27 | 3.16 | 0.05 | 3.36 | 13.03 | 0.42 |
| $2b_2$[a] | 0.521 | 76.30 | 0.10 | 2.62 | 0.0 | 0.0 | 0.0 | 0.0 | 12.41 | 0.40 |
| $13a_1$ | 0.233 | 61.37 | 1.52 | 0.53 | 7.86 | 1.11 | 5.21 | 0.78 | 13.76 | 1.71 |
| $5b_1$ | 0.226 | 61.87 | 5.96 | 0.80 | 0.0 | 0.0 | 0.0 | 0.0 | 10.37 | 0.70 |
| $10e$ | 0.211 | 6.01 | 0.28 | 0.10 | 0.01 | 0.11 | 33.35 | 32.93 | 25.41 | 0.64 |

[a]Highest occupied level.

$N_2 2\pi$ orbital is further reduced (31% of one electron) and it is lying above the $13a_1$ and $5b_1$ Fe $3d$ levels.

From Table IV we can obtain the total amount of metal-to-ligand $\pi$-back-donated charge for each cluster as well as the charge transferred from the $3d_{xy}$ orbital to the $C_eN_e$ groups and from the $3d_{xz,yz}$ to the NO (CO or $N_2$), $C_aN_a$, and $C_eN_e$ groups. On the other hand, the Fe $3d$ charge in the $10e$ orbital can give a rough estimate of the charge back donated to the NO (CO or $N_2$) group. In this way it is possible to classify the ligands in the following sequence of decreasing ability to accept charge from the metal atom:

$$NO^+ >> CO > N_2 \simeq CN^- \ .$$

This ordering is in agreement with previous estimates from experimental data and semiempirical considerations.[1,14–16]

In Table V we are giving the total electron densities at the Fe nucleus for the different clusters as well as the individual contributions from the different iron orbitals. The total charge densities are found to increase in the following sequence:

$$\rho(0)_{Fe(CN)_5N_2^{3-}} < \rho(0)_{Fe(CN)_5CO^{3-}} < \rho(0)_{Fe(CN)_5NO^{2-}} \ .$$

This ordering is clearly the result of an increased $4s$ contribution (Table V). The increase in the $4s$

TABLE IV. Electron population of valence orbitals for the Fe atom in $Fe(CN)_5X$ clusters.

| Orbital | $Fe(CN)_5NO^{2-}$ | $Fe(CN)_5CO^{3-}$ | $Fe(CN)_5N_2^{3-}$ |
|---|---|---|---|
| $3s$ | 1.96 | 1.96 | 1.95 |
| $3p_z$ | 1.92 | 1.93 | 1.93 |
| $3p_{x,y}$ | 3.86 | 3.86 | 3.86 |
| $3d_{z^2}$ | 0.56 | 0.51 | 0.46 |
| $3d_{x^2-y^2}$ | 0.66 | 0.53 | 0.53 |
| $3d_{xz,yz}$ | 2.94 | 3.23 | 3.34 |
| $3d_{xy}$ | 1.82 | 1.72 | 1.72 |
| $4s$ | 1.02 | 0.94 | 0.90 |
| $4p_z$ | 0.73 | 0.59 | 0.50 |
| $4p_{x,y}$ | 0.97 | 0.94 | 0.94 |
| Total charge | | | |
| $3s$ | 1.96 | 1.96 | 1.95 |
| $3p$ | 5.78 | 5.79 | 5.79 |
| $3d$ | 5.98 | 6.00 | 6.06 |
| $4s$ | 1.02 | 0.94 | 0.90 |
| $4p$ | 1.70 | 1.53 | 1.44 |

charge density is due to the decrease in the shielding of the nuclear charge when the $3d$ electrons are removed from the vicinity of the nucleus as a consequence of the back donation of $e$ ($3d_{xz,yz}$) and $b_2$ ($3d_{xy}$) electrons into the $2\pi$ ligand orbitals. As regards the $1s$ and $2s$ orbitals, which lie inside the $3d$ shell, it is expected a decrease in their charge densities when the $3d$ charge is delocalized to the ligands. The $3s$ orbital is largely overlapping the $3d$ orbital and depending on the extension of the $3d$ charge delocalization it may lie inside or outside the $3d$ shell. In the $Fe(CN)_5NO^{2-}$ cluster where the $3d$ charge is strongly delocalized towards the NO group, the $3s$ orbital lies inside the $3d$ shell. It then behaves like the $1s$ and $2s$ orbitals. In the $Fe(CN)_5CO^{3-}$ and $Fe(CN)_5N_2^{3-}$ clusters the $3d$ charge delocalization effect is lower than in the nitrosyl cluster and it is then expected the $3s$ orbital to behave like the $4s$ orbital (Table V). It is thus found that the analysis of the structure of the upper occupied and lower empty energy levels and the total electron densities at the Fe nucleus and the individual orbital contributions indicate a sequence of the $\pi$-acceptor ability of the ligands in full agreement.

The clusters studied are by far not characterized by an Fe $3d^{6+2}$ configuration with $3d_{xz,yz}$ and $3d_{xy}$ orbitals completely occupied. Partial population of the $4s$, $4p$, and $3d_{z^2}$, $3d_{x^2-y^2}$ orbitals leads to a net charge on the Fe atom slightly negative for all the clusters [$Fe(CN)_5NO^{2-}$: $-0.44$, $Fe(CN)_5CO^{3-}$: $-0.22$, $Fe(CN)_5N_2^{3-}$: $-0.14$].

## IV. MÖSSBAUER QUADRUPOLE SPLITTINGS

Assuming that the lattice contribution from neighboring anions and cations is negligible (see Sec. I) the QS energy shift may be written as

$$\Delta E_Q = \tfrac{1}{2} e^2 Q q_{\text{val}} (1 - R) \ , \tag{7}$$

$$q_{\text{val}} = q_{3d} + q_{4p} \ , \tag{8}$$

$$q_{3d} = \tfrac{4}{7} \langle r^{-3} \rangle_{3d} [ (n_{d_{x^2-y^2}} - n_{d_{z^2}}) + (n_{d_{xy}} - n_{d_{xz}(d_{yz})}) ] \ , \tag{9}$$

$$q_{4p} = \tfrac{4}{5} \langle r^{-3} \rangle_{4p} (n_{p_x(p_y)} - n_{p_z}) \ , \tag{10}$$

where $n_{d_{x^2-y^2}}$, etc., are the population of the different Fe $3d$ and $4p$ orbitals (Table IV). The $\langle r^{-3} \rangle_{3d}$ and $\langle r^{-3} \rangle_{4p}$ values were taken from Ref. 27 for the corresponding configuration. The nuclear quadrupole moment $Q$ was taken to be $+0.2$ b.[28] From Table IV we can see that the $3p_z$ and $3p_x(3p_y)$ populations are the same for a given cluster. According to Eq. (10)

TABLE V. Electron charge density (in atomic units) at the iron nucleus for $Fe(CN)_5X$ clusters.

| Orbital | $Fe(CN)_5NO^{2-}$ | $Fe(CN)_5CO^{3-}$ | $Fe(CN)_5N_2^{3-}$ |
|---|---|---|---|
| Fe $1s$ | 10751.980 | 10752.021 | 10752.059 |
| Fe $2s$ | 978.669 | 978.719 | 978.729 |
| Fe $3s$ ($1a_1$) | 139.535 | 139.573 | 139.386 |
| Fe $4s$ ($3a_1 - 12a_1$) | 6.290 | 5.780 | 5.543 |
| Total | 11876.474 | 11876.093 | 11875.717 |

TABLE VI. Experimental and calculated quadrupole splittings for the iron pentacyanide clusters.

| | $Fe(CN)_5NO^{2-}$ | $Fe(CN)_5CO^{3-}$ | $Fe(CN)_5N_2^{3-}$ |
|---|---|---|---|
| $\Delta E_Q$ (expt) (mm/s) | 1.73[a] | 0.43[b] | 0.69[c] |
| $\Delta E_Q$ (calc) (mm/s) | 1.78 | 0.40 | 0.54 |

[a]Reference 14(b). Values quoted in the literature vary from 1.65 to 1.85 mm/s [Ref. 15(b)].
[b]Reference 16.
[c]Reference 17.

we can conclude that the $3p$ core polarization does not significantly contribute to the field gradient at the iron nucleus; i.e., we can neglect the Sternheimer polarization factor in Eq. (7). The same is also true for the Fe $2p$ shell.

In Table VI we are giving the experimental and calculated QS for the different iron(II)-pentacyanide clusters. The calculated values for the $Fe(CN)_5NO^{2-}$ and $Fe(CN)_5CO^{3-}$ clusters agree very well with the experimental data. In the $Fe(CN)_5N_2^{3-}$ cluster the agreement is not so good. We feel that this discrepancy is due to a too short an Fe–$N_2$ distance (see Sec. II) which in turn leads to an overestimation of the $\pi$ back donation into the $N_2$ $2\pi$ orbital.

Our results show that covalency effects involving the Fe $3d$ and $4p$ orbitals play a major role in the calculated EFG and QS energy shifts. The contribution of the $3d$ electrons to the EFG [Eq. (9)] is found to be always positive whereas the $4p$ contribution [Eq. (10)] is always negative. A stronger $\pi$-acceptor ability of the NO (CO or $N_2$) group compared to the CN group ($n_{d_{xz}(d_{yz})} < n_{d_{xy}}$) and the fact that the CN group is a better $\sigma$ donor than the NO (CO or $N_2$) group ($n_{d_{x^2-y^2}} > n_{d_{z^2}}$) can explain the positive contribution of the $3d$ electrons to the field gradient. From Table IV we can see that the $4p_{x,y}$ population is almost the same for all the clusters. $\sigma$ donation from the $C_eN_e$ groups ($5e$ $C_eN_e$ $5\sigma$ level) is the main contribution to the partial occupation of the $4p_{x,y}$ orbitals. Some $\pi$ donation from the $C_aN_a$ and NO (CO or $N_2$) groups may also be found. On the other hand, charge in the $4p_z$ orbital is the result of the $\sigma$ donation from the $C_aN_a$ and NO (CO or $N_2$) groups with some $\pi$ donation from the $C_eN_e$ groups. Because of the unlike symmetry of the overlapping orbitals, no $\sigma$ donation from the $C_eN_e$ into the $4p_z$ orbital and from the $C_aN_a$ or NO (CO or $N_2$) into the $4p_{x,y}$ is expected. Strong $3d$ charge delocalization in the direction of the $z$ axis as a consequence of the $\pi$ back donation seems to favor $\sigma$ donation into the $4p_z$ orbital in the same way as the population of the $4s$ orbital is favored by removing the $3d$ charge from the vicinity of the nucleus (see Sec. III). According to Eq. (10) we finally get a negative contribution to the field gradient. The total EFG ($3d+4p$) is found to be positive for all the clusters which is in agreement with the experimental data.[29]

## ACKNOWLEDGMENTS

The authors are very grateful to Professor J. Danon for many helpful discussions. This work has been supported by the Brazilian agencies FAPESP, FINEP, and CNPq. One of the authors (J.R.L.) is also grateful to the IAE for support.

[1]See, for example, *Mössbauer Spectroscopy,* edited by U. Gonser (Springer, Berlin, 1975); *Mössbauer Spectroscopy and Transition Metal Chemistry,* edited by P. Gütlich, R. Link, and A. Trautwein (Springer, Berlin, 1978).
[2]K. H. Johnson, J. Chem. Phys. 45, 3085 (1966); Adv. Quantum Chem. 7, 143 (1973).
[3]S. Larsson, E. K. Viinika, M. L. de Siqueira, and J. W. D. Connolly, Int. J. Quantum Chem. Symp. 8, 145 (1974); M. L. de Siqueira, S. Larsson, and J. W. D. Connolly, J. Phys. Chem. Solids 36, 1419 (1975).
[4]D. Guenzburger, B. Maffeo, and M. L. de Siqueira, J. Phys. Chem. Solids 38, 35 (1977).
[5]D. Guenzburger, B. Maffeo, and S. Larsson, Int. J. Quantum Chem. 12, 383 (1977).
[6]D. Guenzburger, D. M. S. Esquivel, and J. Danon, Phys. Rev. B 18, 4561 (1978).
[7]C. A. Taft and M. Braga, Phys. Rev. B 21, 5802 (1980).
[8]L. E. Oliveira, B. Maffeo, H. S. Brandi, and M. L. de Siqueira, Phys. Rev. B 13, 2848 (1976).
[9]H. L. Yu, M. L. de Siqueira, and J. W. D. Connolly, Phys. Rev. B 14, 772 (1976).
[10]A. R. Riego, J. R. Leite, and M. L. de Siqueira, Solid State Commun. 31, 25 (1979).
[11]M. Braga, A. R. Riego, and J. Danon, Phys. Rev. B 22, 5128 (1980).
[12]M. Braga and C. A. Taft (unpublished).

[13]M. Braga, S. Larsson, and J. R. Leite, J. Am. Chem. Soc. 101, 3867 (1979); S. Larsson and M. Braga, Int. J. Quantum Chem. 15, 1 (1979).

[14](a) N. L. Costa, J. Danon, and R. M. Xavier, J. Phys. Chem. Solids 23, 1783 (1962); J. Danon, J. Chem. Phys. 41, 3378 (1964); (b) J. Danon and L. Iannarella, *ibid.* 47, 382 (1967).

[15](a) W. Kerler, W. Neuwirth, and E. Fluck, Z. Phys. 173, 321 (1963); 175, 200 (1963); E. Fluck, W. Kerler, and W. Neuwirth, Z. Anorg. Allg. Chem. 333, 235 (1964); 350, 263 (1967); (b) R. W. Grant, R. M. Housley, and U. Gonser, Phys. Rev. 178, 523 (1968).

[16]N. E. Erickson, Ph.D. thesis (University of Washington, Seattle, 1964) (unpublished), p. 90.

[17]K. B. Yatsimirskii, V. V. Nemoshkalenko, Yu. P. Nazarenko, V. G. Aleshin, V. V. Zhilinskaya, and N. A. Tomashevsky, J. Electron Spectrosc. Relat. Phenom. 10, 239 (1977).

[18]P. T. Manoharan and H. B. Gray, J. Am. Chem. Soc. 87, 3340 (1965); J. H. Enermak and R. D. Feltham, Coord. Chem. Rev. 13, 339 (1974).

[19]R. F. Fenske and R. L. DeKock, Inorg. Chem. 11, 437 (1972).

[20]A. Trautwein and F. E. Harris, Theor. Chim. Acta 30, 45 (1973); A. Trautwein, F. E. Harris, and I. Dézsi, *ibid.* 35, 231 (1974); A. Trautwein, R. Reschke, R. Zimmermann, I. Dézsi, and F. E. Harris, J. Phys. (Paris) 35, C6-235 (1974).

[21]K. Schwarz, Phys. Rev. B 5, 2466 (1972).

[22]R. E. Watson, Phys. Rev. 111, 1108 (1958).

[23]L. Pauling, *The Nature of the Chemical Bonding* (Cornell University Press, Ithaca, New York, 1960), p. 221.

[24]F. A. Grimm, T. A. Carlson, W. B. Dress, P. Agron, J. O. Thomson, and J. W. Davenport, J. Chem. Phys. 72, 3041 (1980), and references therein.

[25]A. Tang-Kai and S. Larsson, Int. J. Quantum Chem. 13, 367 (1978).

[26]S. Larsson, Theor. Chim. Acta 49, 45 (1978).

[27]D. M. S. Esquivel, D. Guenzburger, and J. Danon, Phys. Rev. B 19, 1357 (1979).

[28]J. Danon, J. Phys. (Paris) 35, C1-91 (1974).

[29]P. Gütlich, in *Mössbauer Spectroscopy,* edited by U. Gonser (Springer, Berlin, 1975), p. 53; J. Danon, in *IAEA Panel on the Applications of the Mössbauer Effect in Chemistry and Solid State Physics* (International Atomic Energy Agency, Vienna, 1966), p. 89.